Discussions on ANC method

Tae-Sun Park (CENS, IBS)

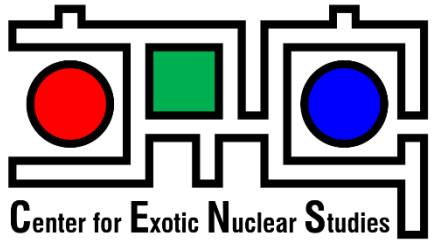

CENS Lunch Seminar, 2020-07-08

Example: $p + 7\mathrm{Be} \rightarrow {}^{8}\mathrm{B} + \gamma$

- Important for the "solar neutrino problem"
  - ${}^{8}\mathrm{B} \rightarrow {}^{8}\mathrm{Be}^{*} + e^{+} + \nu_e$ produces about only 0.02% of solar neutrinos, but neutrinos of energy up to 15 MeV

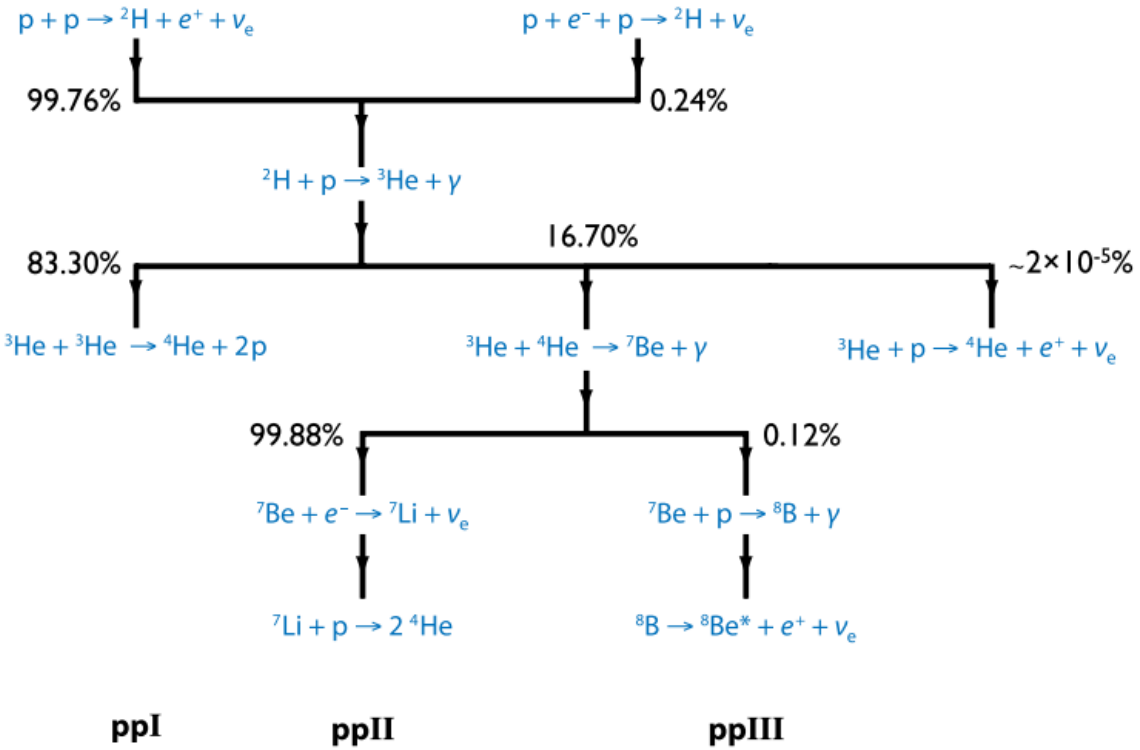

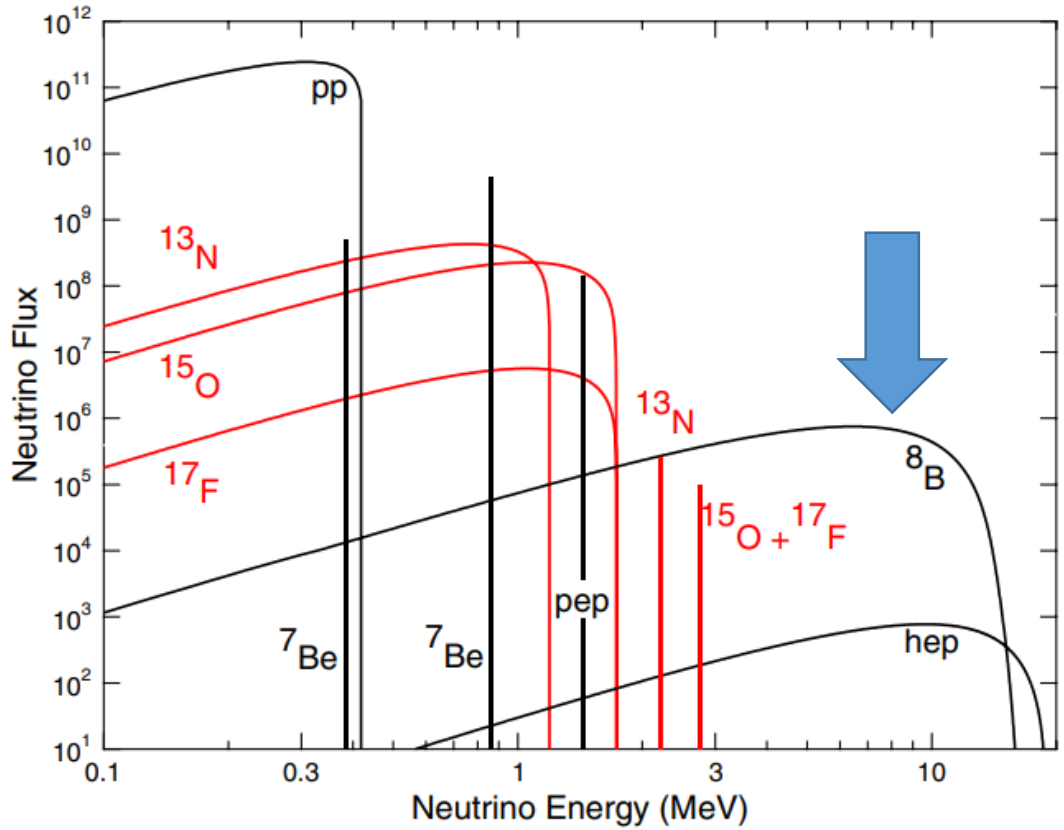

Rev. Mod. Phys. 83 (2011) 195

- Need to know $S_{17}(\mathrm{E}) = E\ \mathrm{e}^{2\pi\eta}\ \sigma(E\ )$ of $p + 7\mathrm{Be} \rightarrow {}^{8}\mathrm{B} + \gamma$ at $E < 20$ keV, or $\boldsymbol{S_{17}(0)}, S'_{17}(0), \ldots.$
- Direct experiments are difficult at such a low-energy, and requires extrapolation.
- One possibility is the Coulomb Dissociation method (which involves E1 & E2)

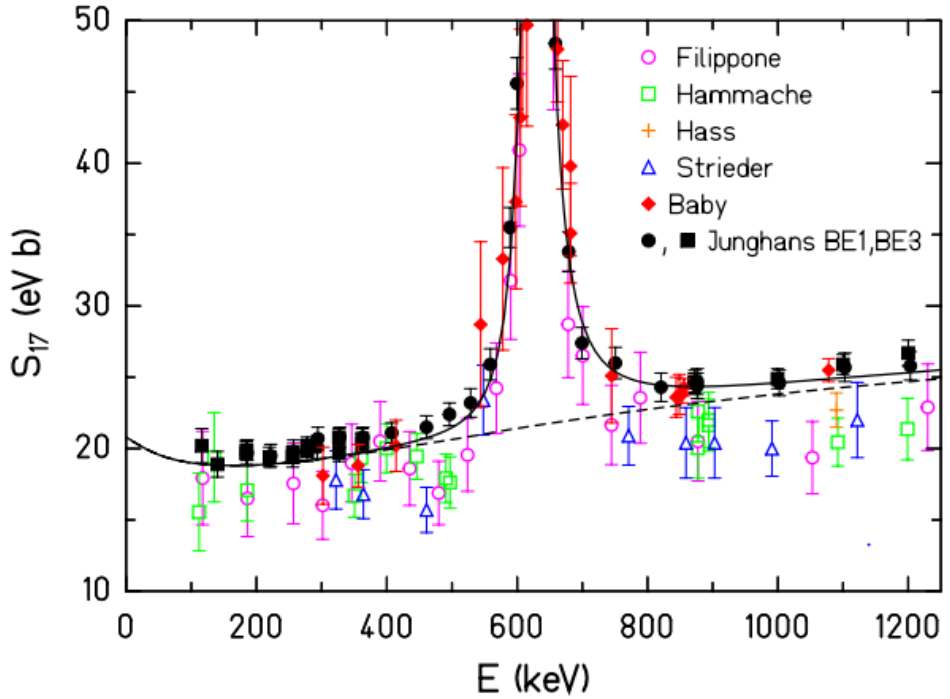

FIG. 9 (color online). $S_{17}(E)$ vs center-of-mass energy E, for $E \leq$ 1250 keV. Data points are shown with total errors, including systematic errors. Dashed line: scaled Descouvemont (2004) curve with $S_{17}(0) = 20.8$ eV b; solid line: including a fitted 1^+ resonance shape.

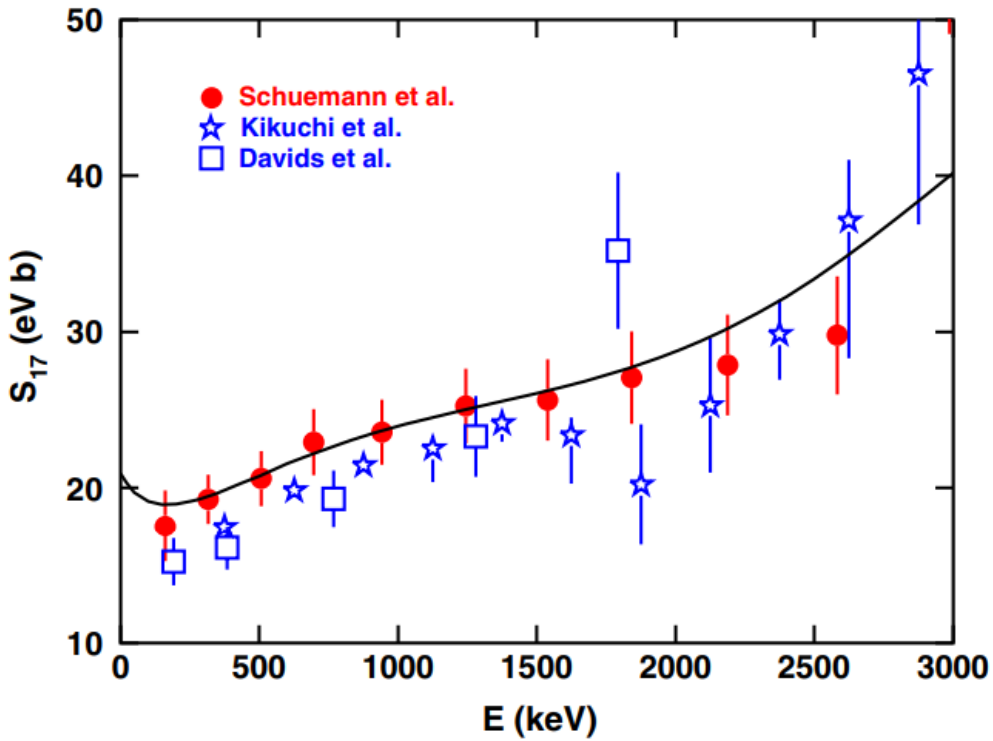

FIG. 8 (color online). S_{17} values from CD experiments. Full circles: latest analysis of the GSI CD experiment (Schümann *et al.*, 2006); open stars: Kikuchi *et al.* (1998) analyzed in first-order perturbation theory; open squares: Davids and Typel (2003).

Typical indirect methods

- Coulomb Dissociation
- Trojan Horse method
- **Asymptotic Normalization Constant (ANC)**

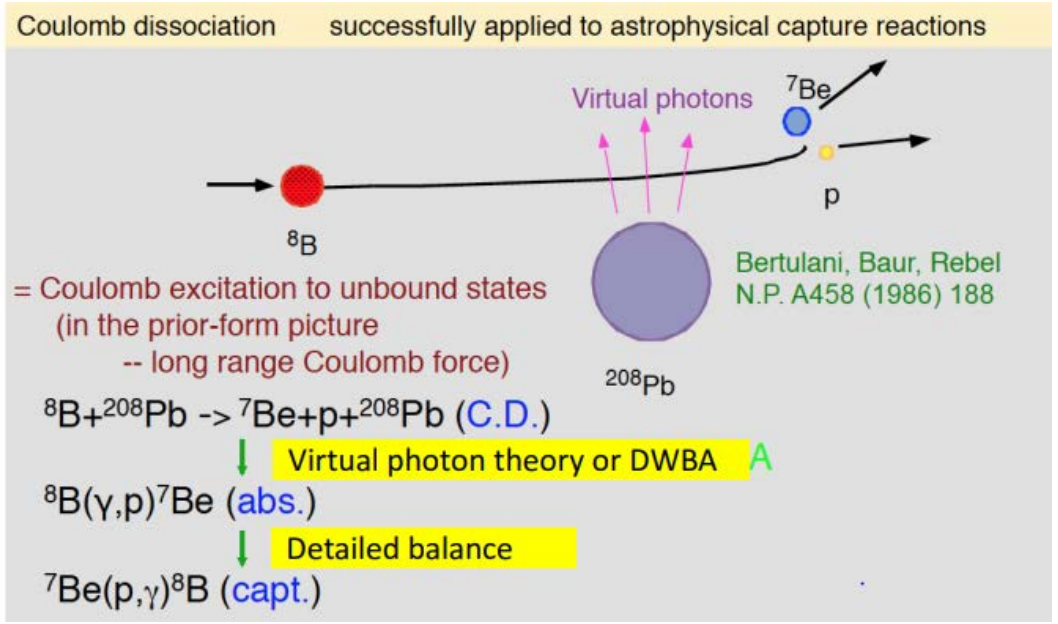

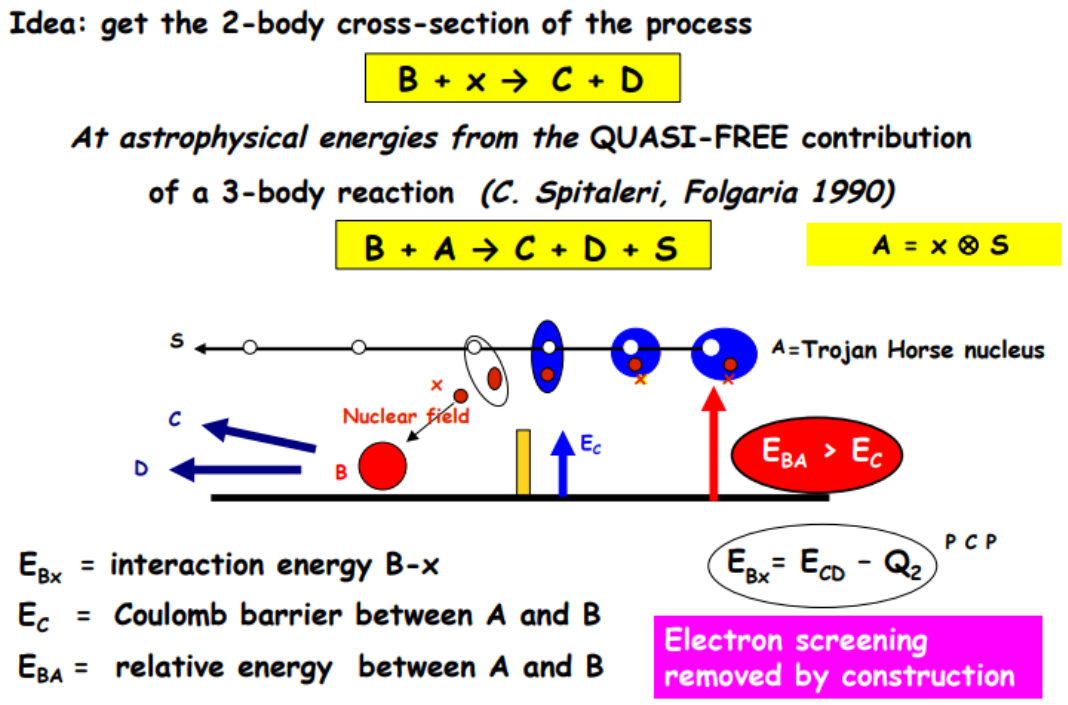

- Another possibility is ANC method
  - BE=0.1375 MeV; $\mathrm{k} = \sqrt{2\mu\, BE} = 15\, MeV$,
  - $\frac{1}{k} = 13$ fm $\gg R_N \approx 3$ fm, peripheral
  - 8B is a loosely bund system of p+7Be.
- Matrix element for $p + 7\mathrm{Be} \rightarrow {}^{8}\mathrm{B} + \gamma$

$$\sim \int d\boldsymbol{r}\, \Psi^{*}_{8B}\ \boldsymbol{\varepsilon}\cdot\boldsymbol{J}(r)\, e^{i\boldsymbol{k}\cdot\boldsymbol{r}}\, \Psi_{p+7Be}$$

$$\propto \int_0^{\infty} dr \cdot r \cdot I_{p+7\mathrm{Be}\rightarrow{}^{8}\mathrm{B}+\gamma}\,(r)$$

  - Dominated by
    - $\Psi_{p+7Be} \sim \frac{1}{r}\ F_L\,(\eta, kr+\delta)\ \phi_p\ \phi_{7Be}\ Y_{LM},\ \ \mathrm{L} = 1, \delta \simeq 0$
    - $\Psi_{8B} \sim C_{ANC}\ \frac{1}{r}\ W_L\,(\eta, kr)\ \phi_p\ \phi_{7Be}\ Y_{LM}$
    - $I_{p+7\mathrm{Be}\rightarrow{}^{8}\mathrm{B}+\gamma}(r) \sim C_{ANC}\ F_L\,(\eta, kr)\ W_L\,(\eta, kr)$
  - F & W: Coulomb & Whittacker ftns: Solution of radial Schrodinger equation with Coulomb potential. E>0 and E<0.
  - The only unknown quantity: C_{ANC}, the asymptotic normalization constant
  - C_{ANC} may be theoretically evaluated by a microscopic calculation (Quantum Monte-Carlo Green's function, No-Core Shell-Model, …)

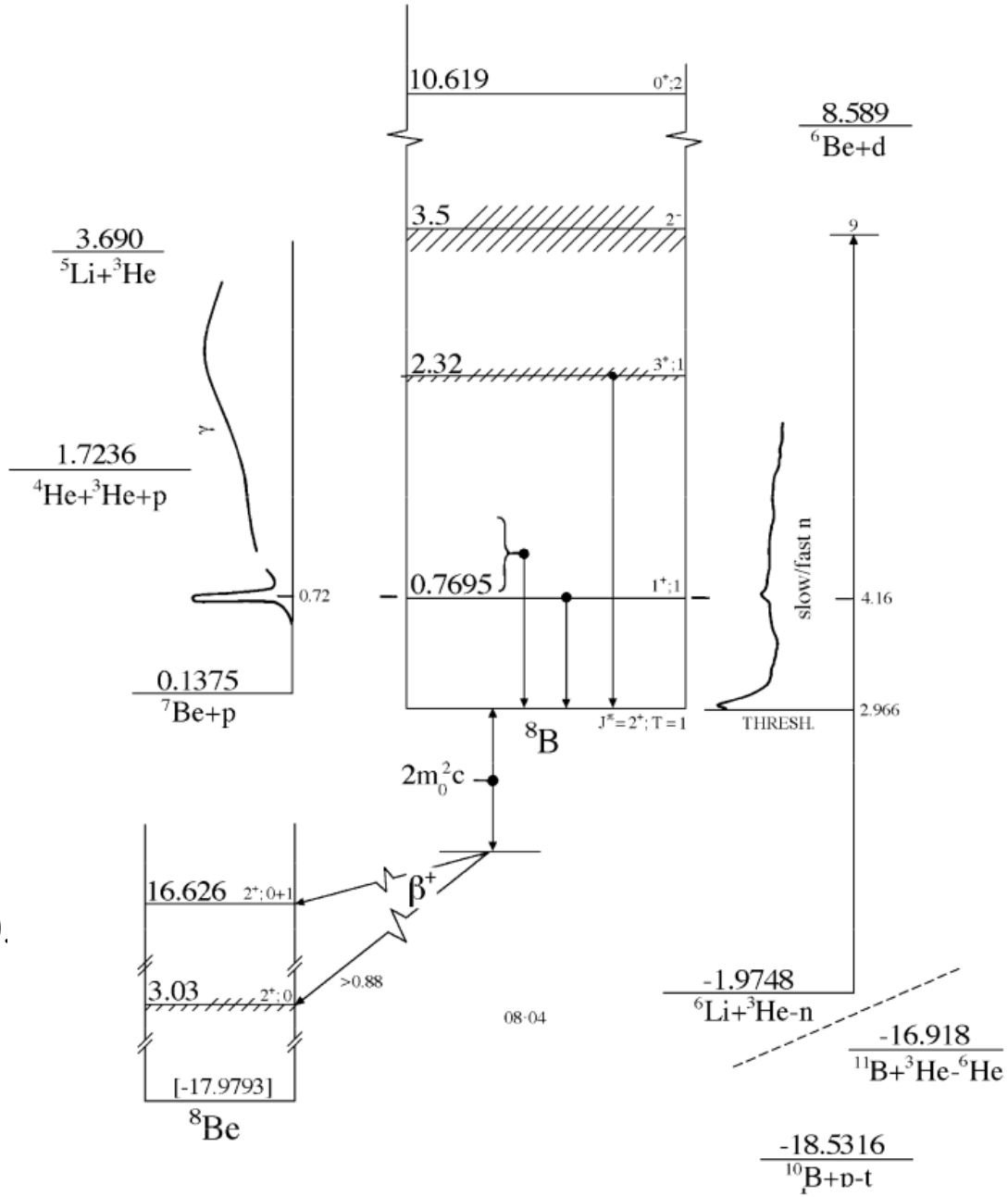

Fig. 4. Energy levels of ^{8}B. For notation see Fig. 2.

To be more precise, $|\Psi_{^8B}\rangle = |\Psi_{p+^7Be}\rangle \oplus |\Psi_{^7Li+^3He}\rangle \oplus |\Psi_{p+\alpha+^3He}\rangle \oplus \cdots$

⊛ Let $\vec{r} = \vec{r}_{p-^7Be}$,

$$\lim_{r\to\infty} \Psi_{^8B}(\vec{r}_1,\vec{r}_2,\cdots) = \sum_{L_p, J_p} \Big[\Big[Y_{L_p}(\hat{r}) \otimes \phi_p^{S_p=\frac{1}{2}} \Big]^{J_p} \otimes \phi_{^7Be}^{S_1=\frac{3}{2}} \Big]^{J J_Z} \cdot I_{17;L_p J_p}(r)$$

($L_p = 1$? $J_p = \{\frac{1}{2}, \frac{3}{2}\}$)

$I_{17;L_p J_p}(r)$ = $I^{^8B}_{p+^7Be, L_p J_p}(r)$

$$I_{17;L_p J_p}(r) = \sqrt{S_{17;L_p J_p}} \cdot \frac{1}{r} u_{17;L_p J_p}(r),$$

$$\int_0^\infty |u_{17;L_p J_p}(r)|^2 dr = 1.$$

$$\lim_{r\to\infty} u_{17;L_p J_p}(r) = \beta_{17;L_p J_p} \underbrace{W_{L_p}(\eta, kr)}_{\approx e^{-kr}}$$

$$\lim_{r\to\infty} I_{17;L_p J_p}(r) = C_{17;L_p J_p} \cdot \frac{1}{r} W_{L_p}(\eta, kr)$$

with $C_{17;L_p J_p} = \sqrt{S_{17;L_p J_p}} \cdot \beta_{17;L_p J_p}$ = Asymp. normal. const. (ANC).

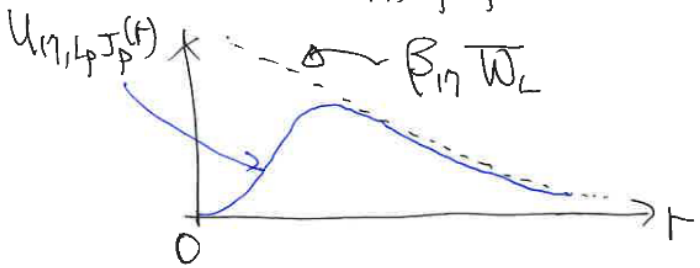

$$\left[-\frac{\nabla^2}{2\mu} + \frac{Z_1 Z_2 \alpha_{EM}}{r} \right] \frac{u(r)}{r} Y_{LM} = E \cdot \frac{u(r)}{r} Y_{LM},$$

$$\rightarrow \quad u(r) = \begin{cases} F_L(\eta, kr) \text{ and } G_L(\eta, kr), & E>0,\ k=\sqrt{2\mu E} \\ W_L(\eta, kr), & E<0,\ k=\sqrt{2\mu|E|} \end{cases}$$

with $\eta = \frac{Z_1 Z_2 \alpha_{EM}}{v/c}$, $\alpha_{EM} = \frac{e^2}{\hbar c} = \frac{1}{137.036\cdots}$,

$F_L \sim \sin(kr)$, $G_L \sim \cos(kr)$, $W_L \sim e^{-kr}$ when $\eta \to 0$.

* Initial scattering $p + {}^7Be$ w.f.

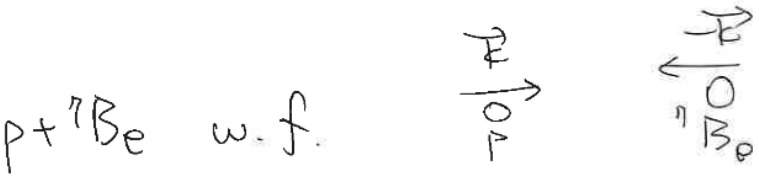

$$\Psi_{in}(\vec{r}_1, \vec{r}_2, \dots) = \left[e^{i\vec{k}\cdot\vec{r}} \; \phi_p^{s_p,\mu_p} \; \phi_7^{s_7,\mu_7} \right]_{\oplus} = \text{"C"} + \text{"N"}$$

$$= \left[4\pi \sum_{LL_z} i^L Y_{LL_z}(\hat{r}) \, Y^*_{LL_z}(\hat{k}) \, j_L(kr) \; \phi_p \; \phi_7 \right]_+$$

$$= \left[4\pi \sum_{LL_z} i^L Y_{LL_z}(\hat{r}) \, Y^*_{LL_z}(\hat{k}) \, e^{i\delta_L} \frac{F_L(\eta, kr)}{r} \; \phi_p \, \phi_7 \right]_{+N}$$

$= \dots$

$$\simeq 4\pi \sum_{LL_z} i^L Y_{LL_z}(\hat{r}) \, Y^*_{LL_z}(\hat{k}) \, e^{i\delta_L} \frac{u_{in,L}(r)}{r} \; \phi_p \, \phi_7$$

$$u_{in,L}(r) \underset{r > R_N}{\simeq} F_L(\eta, kr + \delta_L) \overset{\delta_L \simeq 0 \text{ at } k \to 0}{\simeq} F_L(\eta, kr) \sim i^L \sin(kr) \text{ at } \eta = 0.$$

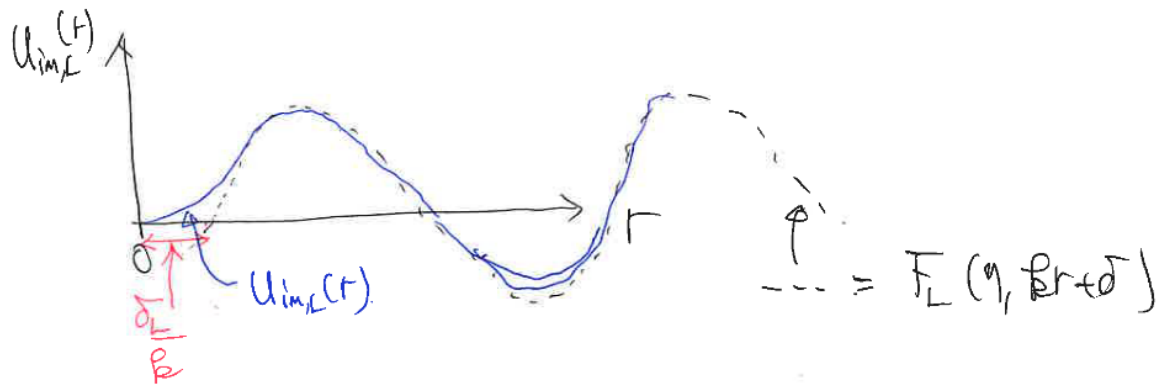

⊛ Matrix element of $p + {}^7Be \to {}^8B + \gamma$:

$\hat{\mathcal{O}}_{E1} \propto r$

$$\mathcal{M} = \langle \Psi_{^8B} | \hat{\mathcal{O}} | \Psi_{im} \rangle \approx \langle \Psi_{^8B} | \hat{\mathcal{O}}_{E1} | \Psi_{im} \rangle$$

$$\propto \sum_{L_p J_p} \int d^3\vec{r} \; I_{I_7; L_p J_p}(r) \cdot \hat{\mathcal{O}}_{E1}(r) \cdot e^{i\delta_L} \frac{u_{im; L_p}(r)}{r}$$

$$\propto \sum_{L_p, J_p} \sqrt{\ell_{I_7; L_p J_p}} \int_0^\infty dr \cdot u_{I_7; L_p J_p}(r) \cdot r \cdot u_{im; L_p}(r) \qquad /// \; \mathcal{M}_{L_p J_p}$$

$$\approx \sum_{L_p, J_p} \sqrt{\ell_{I_7; L_p J_p}} \cdot \beta_{I_7; L_p J_p} \int_{R_{cut}}^\infty dr \cdot W_{L_p}(\eta, \rho_r) \cdot r \cdot F_{L_p}(\eta, \rho_r)$$

$$= \sum_{L_p J_p} C_{I_7; L_p J_p} \cdot \frac{\mathcal{M}_{L_p J_p}}{\beta_{I_7; L_p J_p}} \leftarrow \text{model-indep.}$$

$$\frac{d\sigma}{d\Omega} = \sum_{L_p, J_p} \left| C_{I_7; L_p J_p} \right|^2 \cdot \frac{d\sigma_{L_p J_p}}{\beta^2_{I_7; L_p J_p}}$$

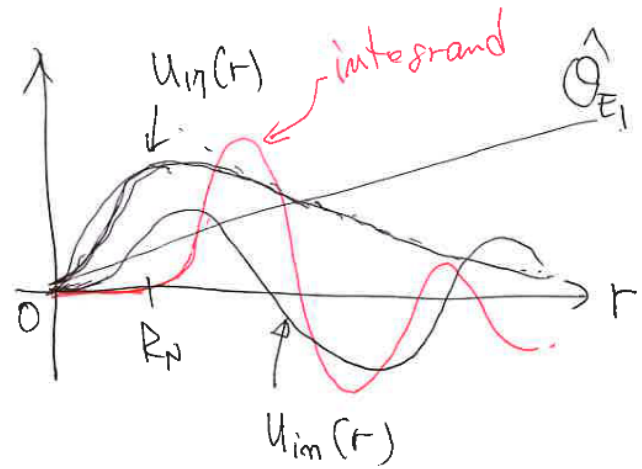

How can we get C_{ANC}? (I)

- $^{7}\mathrm{Be}(a,b)^{8}\mathrm{B}$ with $a = b + p$ is handy !
  - Amp ~ $C^{8B}_{p+7Be}\, C^{a}_{b+p}\, \frac{1}{|\vec{k}-\vec{k}'|^2}$ (peak at forward angle)
  - We can use DWBA or CC codes to calculate amplitudes with ANCs
- Oops, but we then need another ANC, C^{a}_{b+p} !
- How to get C^{a}_{b+p} ?
  - Using simple systems, e.g. $^{7}\mathrm{Be}(\mathrm{D},\mathrm{n})^{8}\mathrm{B}$ and $^{7}\mathrm{Be}(^{3}\mathrm{He},\mathrm{D})^{8}\mathrm{B}$
  - Or by $a(b,a)b$ with $a = b + p$.That is, $^{10}\mathrm{B}(^{7}\mathrm{Be},^{8}\mathrm{B})^{9}\mathrm{Be}$ and $^{9}\mathrm{Be}(^{10}\mathrm{B},^{9}\mathrm{Be})^{10}\mathrm{B}$
- PRC56 ('97) 1302: $^{9}\mathrm{Be}(^{10}\mathrm{B},^{9}\mathrm{Be})^{10}\mathrm{B}$ at E=100 MeV

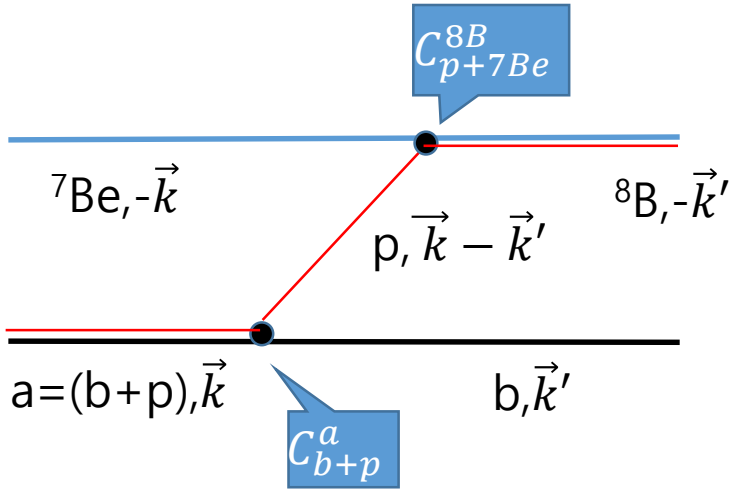

+ ...

How can we get C_{ANC} ? (I)

- PRC56 ('97) 1302: $^{9}Be(^{10}B, ^{9}Be)^{10}B$ at E=100 MeV

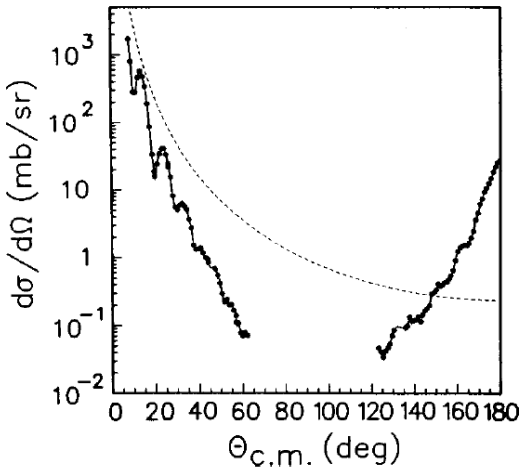

FIG. 3. The angular distribution for elastic scattering of 100 MeV ^{10}B on ^{9}Be is shown over the whole angular range $\theta_{c.m.}=0°-180°$. The data at forward angles were obtained by measuring the elastically scattered ^{10}B nuclei. Those at backward

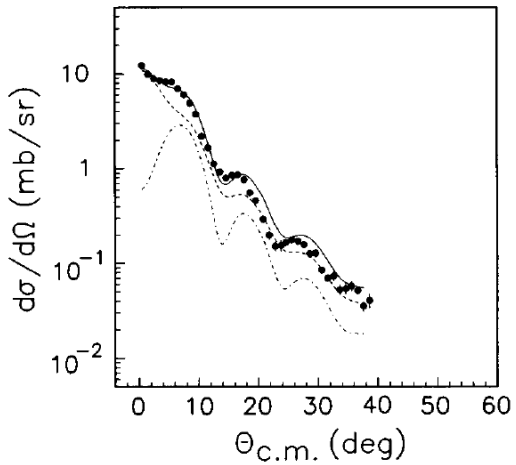

FIG. 6. The experimental and calculated angular distributions for the reaction $^{9}Be(^{10}B,^{9}Be)^{10}B(0.718$ MeV). The points are experimental data; the solid line is the DWBA fit. The dashed line is

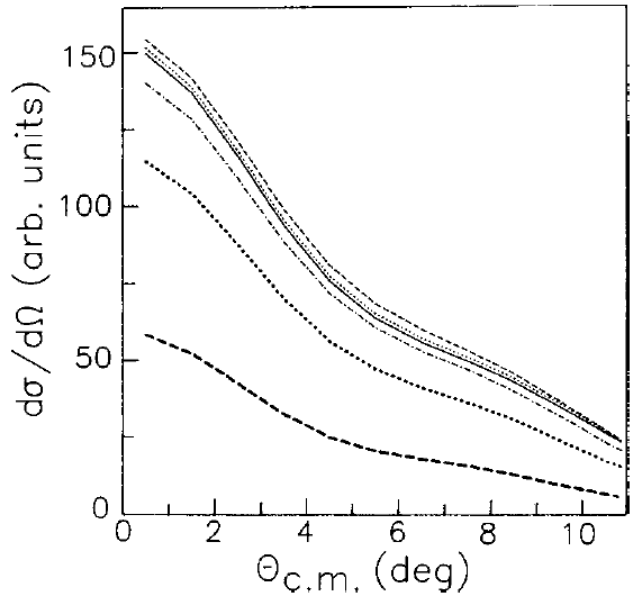

FIG. 9. The dependence of the DWBA differential cross section on the cutoff radius. The lines are the DWBA cross sections for the reaction $^{9}Be(^{10}B,^{9}Be)^{10}B$ for different cutoff radii: the solid line is for $R_{cut}=0$ fm, the light dotted line for $R_{cut}=4.0$ fm, the light dashed line for $R_{cut}=5.0$ fm, the light dashed-dotted line for $R_{cut}=5.5$ fm, the dark dotted line for $R_{cut}=6.0$ fm, the dark dashed line for $R_{cut}=7.0$ fm. The calculations have been done with the geometric parameters of the bound state Woods-Saxon potential $r_0=1.20$ fm, $a=0.60$ fm, and optical potential 1. Optical potential 2 gives similar results.

TABLE I. The parameters of the Woods-Saxon optical model potentials extracted from the analysis of the elastic scattering data for ^{10}B (100 MeV)+^{9}Be. We use standard notations: V and W are the depths of the real and imaginary (volume) potentials, r_V, a_V are the radius and diffuseness parameters of the real potential, and r_W, a_W are the radius and diffuseness parameters of the imaginary potential. The Coulomb radius parameter is $r_C=1.0$ fm for all potentials.

Pot.	V [MeV]	W [MeV]	r_V [fm]	r_W [fm]	a_V [fm]	a_W [fm]	χ^2	σ_R [mb]	J_V [MeVfm3]	J_W [MeV fm^3]
1	64.2	30.1	0.78	0.99	0.99	0.75	19.8	1318	206	136
2	131.2	29.7	0.67	0.95	0.90	0.86	45.4	1411	276	131
3	203.2	24.7	0.81	1.04	0.60	0.83	61.8	1428	499	133

How can we get C_{ANC} ? (I)

- PRC56 ('97) 1302: $^{9}Be(^{10}B, ^{9}Be)^{10}B$ at E=100 MeV

TABLE II. Dependence of the DWBA cross section and R function on b for the reaction $^{9}Be(^{10}B,^{9}Be)^{10}B$(g.s.). The calculations have been done with optical potential 1 at a scattering angle $\theta=0°$; r_0 and a are the geometric parameters of the bound state Woods-Saxon potentials. The Coulomb radius parameter is 1.2 fm.

r_0 [fm]	a [fm]	b [fm$^{-1/2}$]	C^2 [fm^{-1}]	$d\sigma^{DW}/d\Omega$ [mb/sr]	R
1.1	0.5	2.50	4.52	52.34	1.35
1.1	0.7	3.12	4.87	117.38	1.25
1.2	0.6	3.01	4.78	107.01	1.30
1.3	0.5	2.98	4.73	104.01	1.33
1.3	0.7	3.61	5.00	201.43	1.18

$$\frac{d\sigma}{d\Omega}=\sum_{j_B j_X}(C^{B}_{Aal_Bj_B})^2(C^{X}_{Yal_Xj_X})^2R_{l_Bj_Bl_Xj_X},$$

where

$$R_{l_Bj_Bl_Xj_X}=\frac{\sigma^{DW}_{l_Bj_Bl_Xj_X}}{b^2_{Aal_Bj_B}b^2_{Yal_Xj_X}}$$

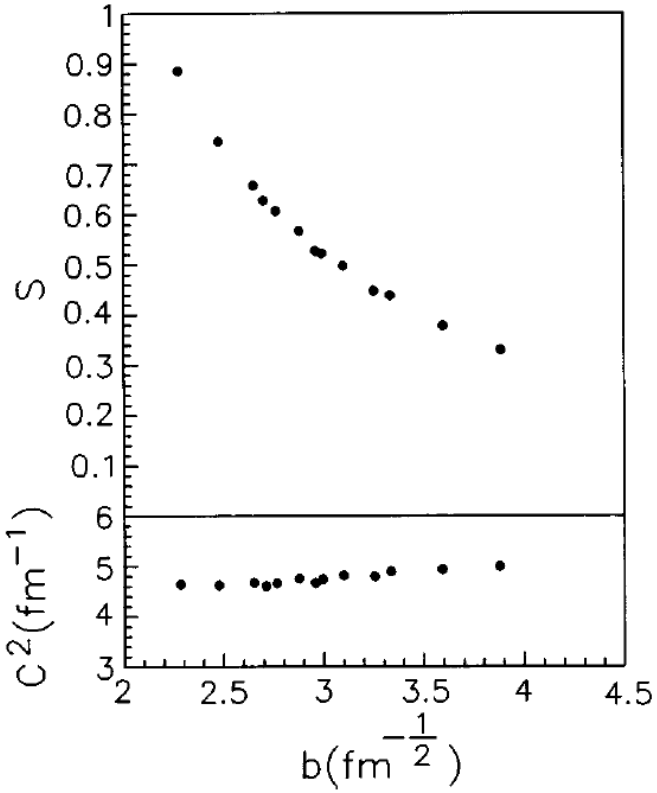

FIG. 11. The upper panel shows the dependence of the extracted spectroscopic factor S for the configuration $^{9}Be(3/2^-)+p(j_p=3/2^-)$ in ^{10}B(g.s.) on the single-particle ANC b. The lower panel shows the extracted ANC C^2 of the associated overlap function for the same values of b. Both calculations have been done using optical potential 1.

Errors in C_{ANC} ?

- Dependence on optical pot. parameters : ~5%
- Multi-step: ~ 3%
- DWBA vs Coupled-channel ~ 3%
- Peripheral condition: satisfied ($k\ R_{ch} = 16$) for $R_{ch} = 5$ fm

- In total, they assigned ± 9 % in C^2,

  $C^2 = 5.06 \pm 0.46$ [fm]

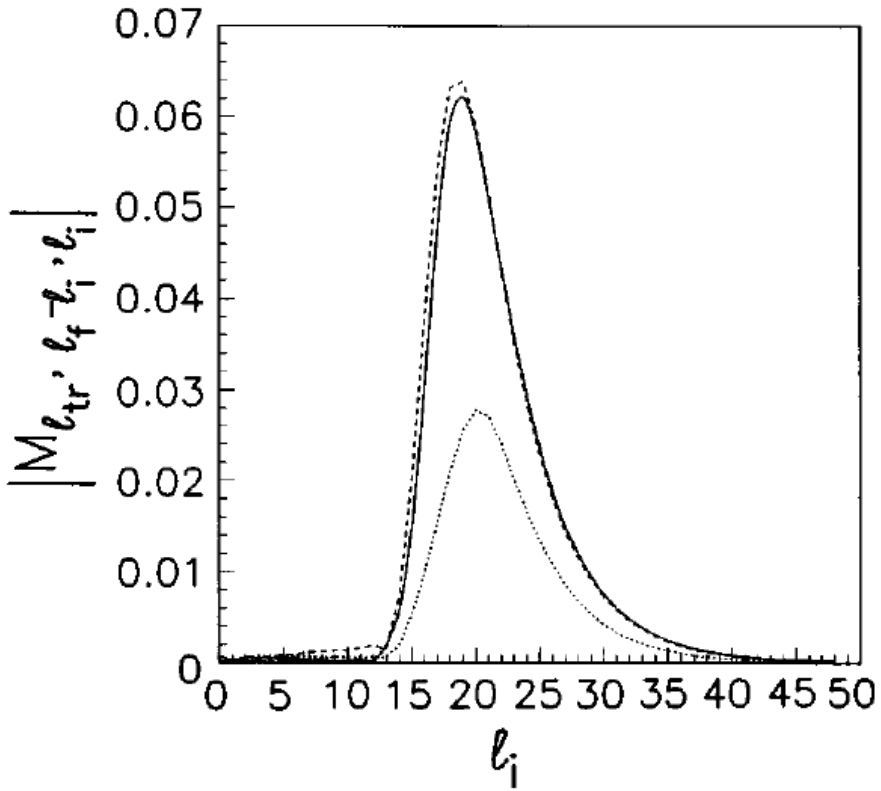

FIG. 12. The l_i dependence of the modulus of the partial wave reaction amplitudes $M_{l_{tr}, l_f - l_i, l_i}$ for the reaction ^{9}Be(^{10}B,^{9}Be)^{10}B at different l_{tr}. Here l_i and l_f are the relative orbital angular momenta of the ^{10}B and ^{9}Be nuclei in the entrance and exit channels, respectively. The solid line is for $l_{tr}=0$, $l_f - l_i = 0$; the dashed line is for $l_{tr}=1$, $l_f - l_i = 0$; and the dotted line is for $l_{tr}=2$, $l_f - l_i = -2$. In the latter case, the contributions with $l_f - l_i = 0$ and $+2$ are comparable to the one shown.

Errors in C_{ANC} ?

- Fernandes et al, PRC59('99)2865.
  - A careful examination of S_{17}

We conclude that the ANC method to extract the S factor from the transfer using the DWBA is accurate to 8% if the optical potentials for the incoming and outgoing channels are well defined, have no strong surface peaked potentials, and the reaction is clearly peripheral. More measurements at the

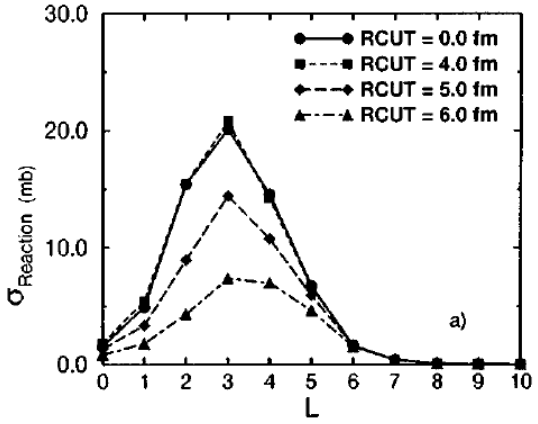

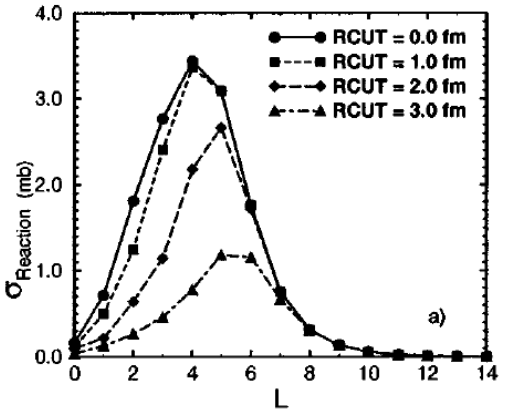

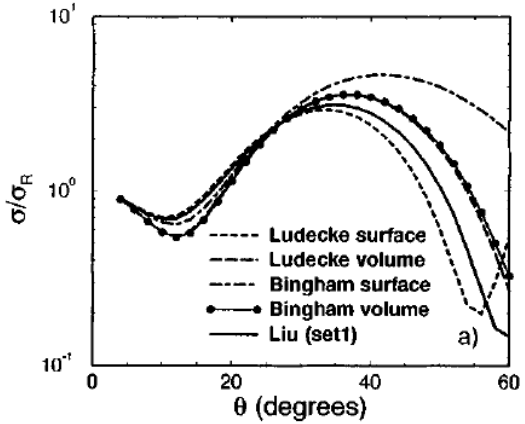

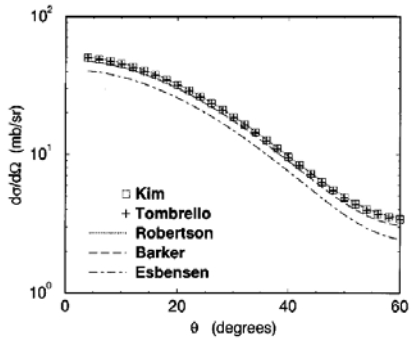

FIG. 5. Calculated differential cross section for the ^{7}Be$(d,n)^{8}$B reaction using different models for the ^{8}B g.s. at $E_{c.m.}$=5.8 MeV.

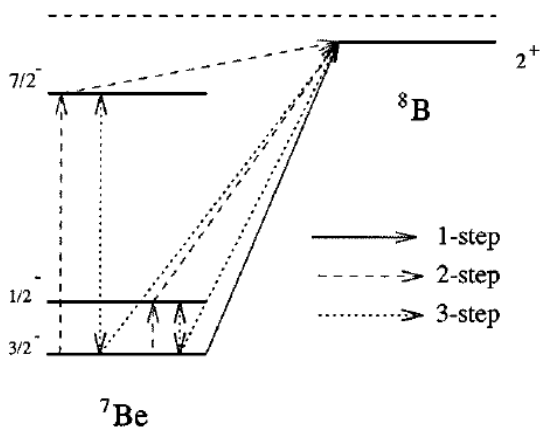

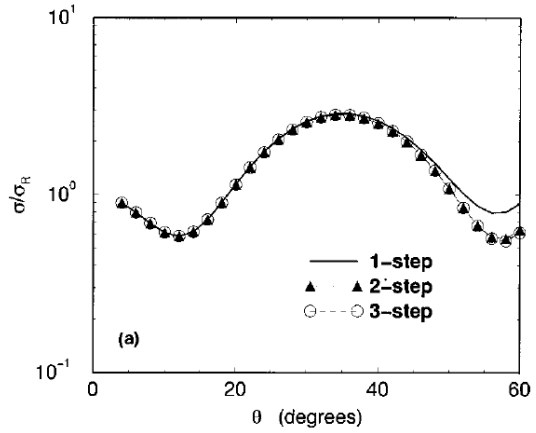

Errors in C_{ANC} ?

- Fernandes et al, PRC61('99)064616.
  - ^{10}B -> ^{9}Be + p

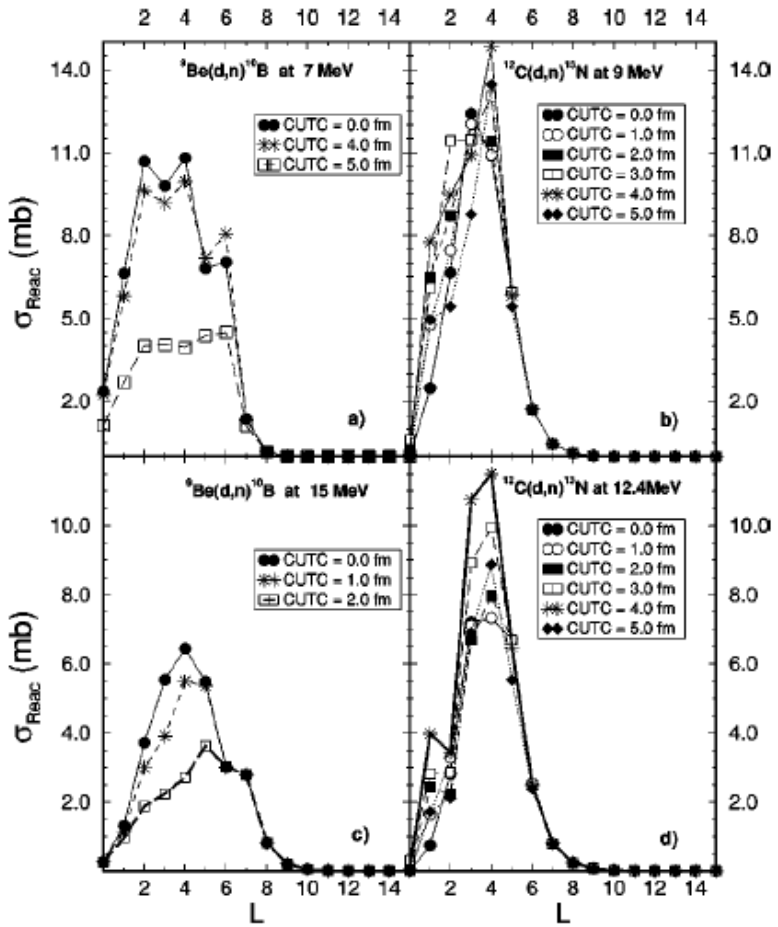

FIG. 11. Calculated reaction cross section for each partial wave L for ^{9}Be$(d,n)^{10}$B at 7 and 15 MeV, and ^{12}C$(d,n)^{13}$N reactions at 9 and 12.4 MeV.

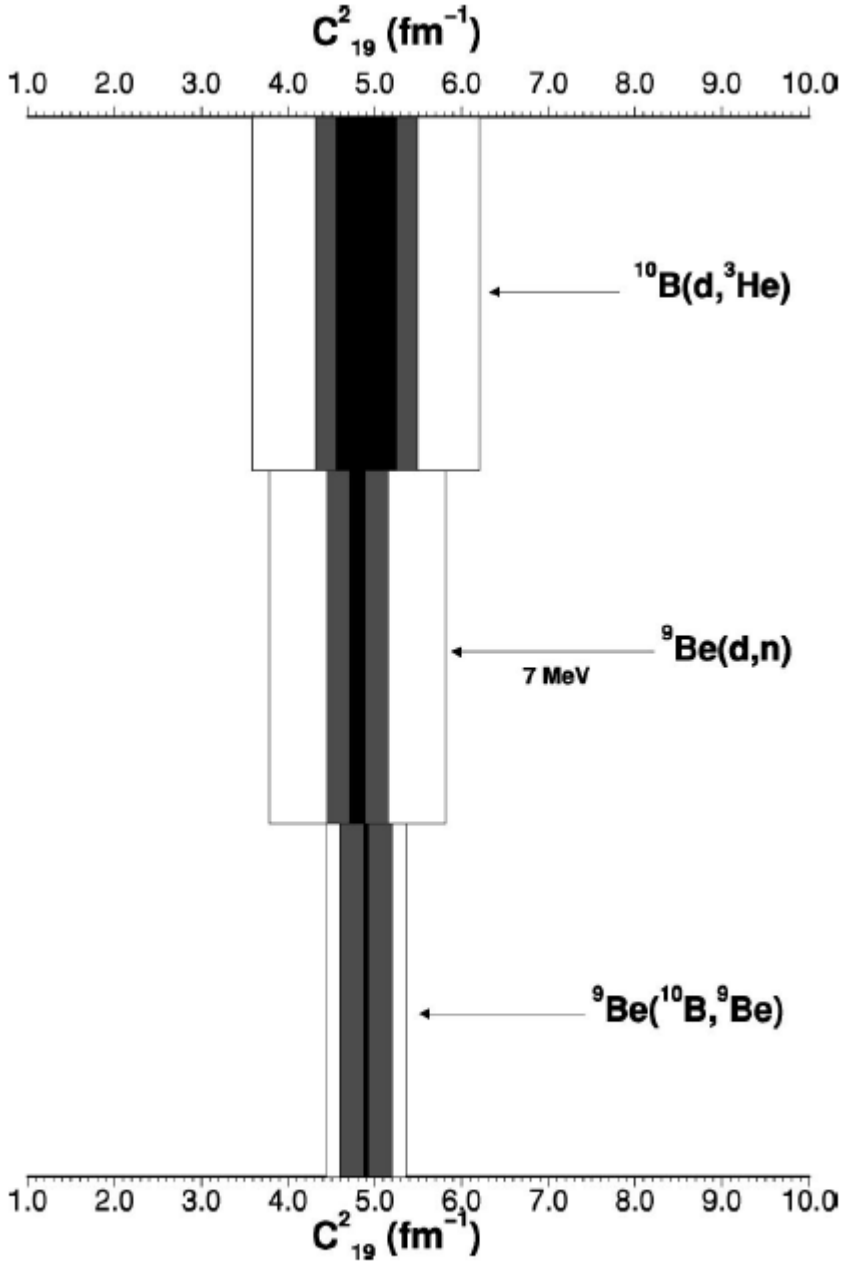

FIG. 8. Sum of the contributions of the statistical (dark bar), optical potential (light grey bar), and systematic (white bar) uncertainties for the calculated ANC's.

How can we get C_{ANC} ? (II)

$$S(E) = \sum_{j_B} C^2_{Aa;l_B j_B} R_{l_B j_B}(E, b_{Aa;l_B j_B}),$$

where

$$R_{l_B j_B}(E, b_{l_B j_B}) = \frac{\tilde{S}_{l_B j_B}(E)}{b^2_{Aa;l_B j_B}}.$$

- If we know ANC, we can find S-factors.
- => If we know S-factors, we can extract ANC
- NPA 781('07)247:
  - The $R_{lbjB}(E)$ can be calculated by rather reliably by DWBA
    - Independent on b (details)
  - It then allows us to extract C for each E
  - C is E-independent, we can deduce S(0)

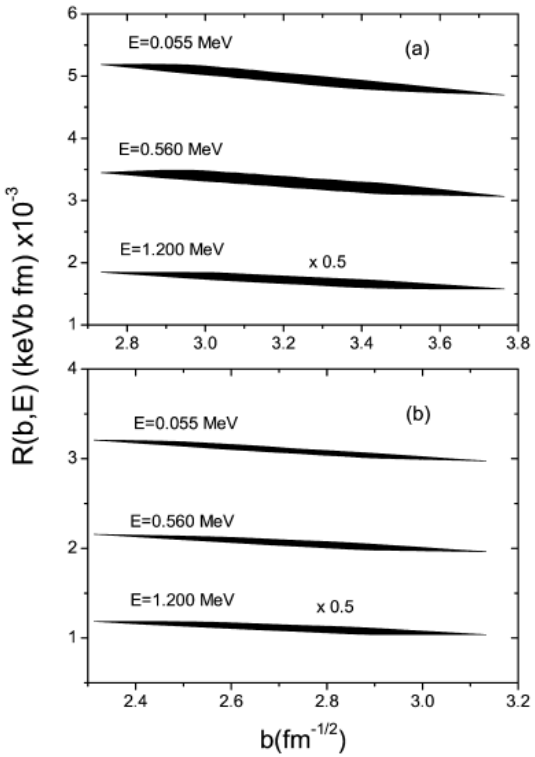

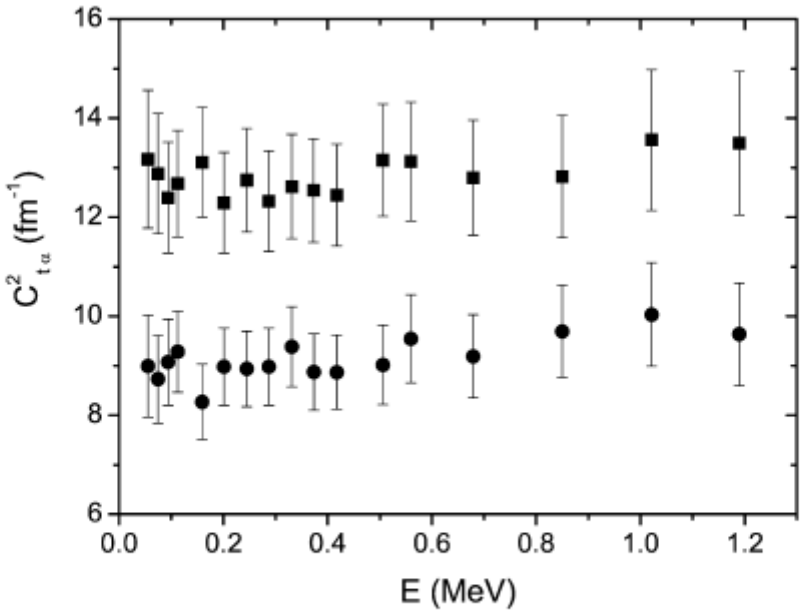

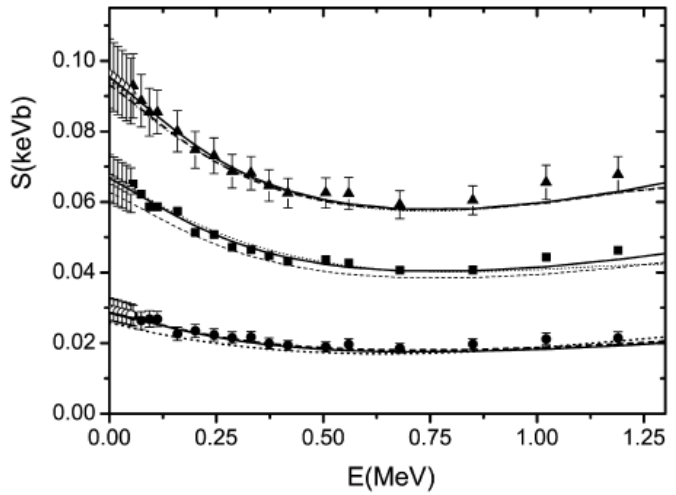

trophysical S-factors for the $t + \alpha \rightarrow {}^7\mathrm{Li(g.s.)} + \gamma$ (square), $t + \alpha \rightarrow {}^7\mathrm{Li(0.478\ MeV)} + \gamma$ (ci
g.s. + 0.478 MeV) + γ (triangles) reactions. The filled symbols are experimental data taken fron
uts are our results. The solid lines are the results of our calculation with the standard values of r_o :
fm, the dashed lines are the results of Ref. [23] and the dotted lines are the results of Ref. [21].

Fig. 5. The values of the ANC's, $C^2_{t\alpha}$ and $(C^*_{t\alpha})^2$, for the $\alpha + t \rightarrow {}^7\mathrm{Li}$ at all experimental energies E_i. The square (circle) symbols are for the ground (excited ($E^* = 0.478$ MeV)) state of ^{7}Li.

How can we get C_{ANC} ? (III) ERE with phase-shifts

- Elastic scattering:
  - It is s-channel (among s,t,u), hard to extract by angle-dependence
  - Amplitude has a simple-pole at $E = -\varepsilon$,
  - $S_l \sim (-)^{L+1} i\, e^{-\pi\eta} \frac{C^2}{k - i\kappa} + \cdots$,Blokhintsev et al. SJPN 1984
  - Example: PRC84('11)024603 & (PRC96 ('17) 034601 for 12C+a)
    - (partial wave analysis) -> (δ_L) →
    - (effective range expansion: $k^{2L+1} \cot \delta_L = -\frac{1}{a} + \frac{r}{2} k^2 - P\, r^3 k^4 + \cdots$
    - C^2 in terms of $(a, r, P, \cdots)$

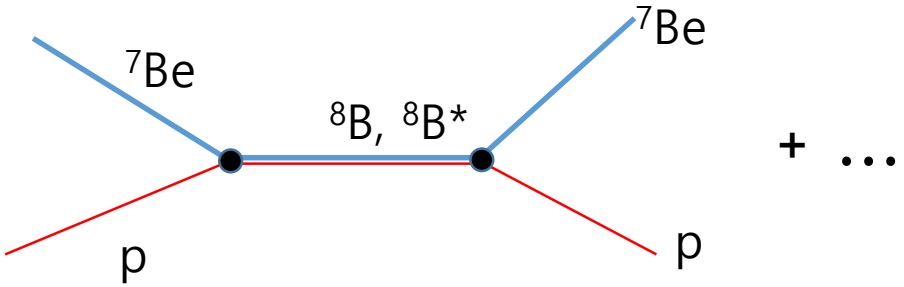

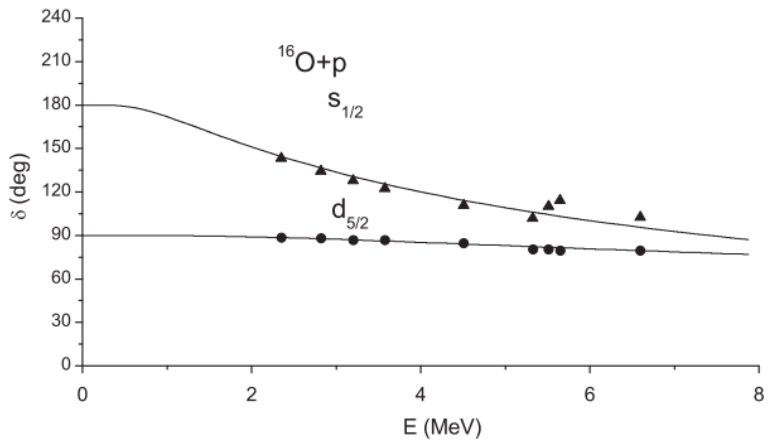

FIG. 2. $s1/2$ and $d5/2$ $^{16}\mathrm{O} + p$ phase shifts. The curves display results obtained from the effective-range expansion with parameters from Table I. Triangles $(s_{1/2})$ and circles $(d_{5/2})$ represent experimental values of Ref. [21]. The $d_{5/2}$ phase shifts are shifted by 90° for clarity.

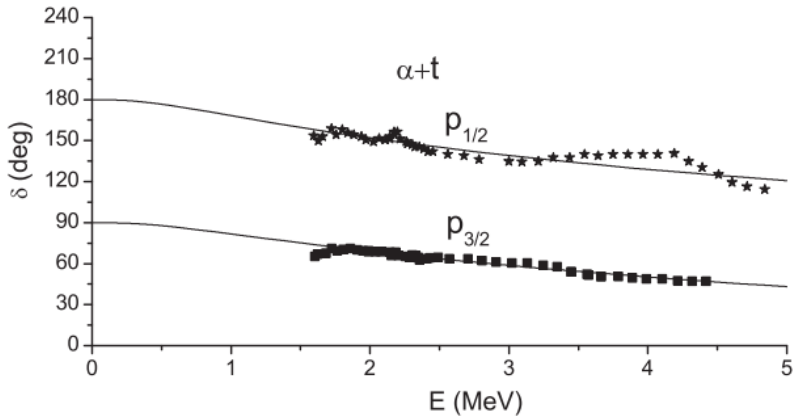

FIG. 5. $p1/2$ and $p3/2$ $\alpha + t$ phase shifts. The curves display results obtained from the effective-range expansion with parameters from Table I. Stars $(p_{1/2})$ and squares $(p_{3/2})$ represent experimental values of Ref. [22]. The $p_{3/2}$ phase shifts are shifted by 90° for clarity.

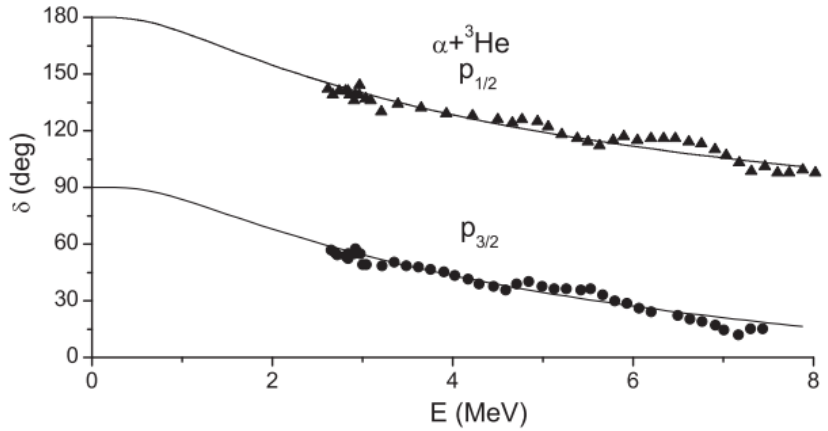

FIG. 6. $p1/2$ and $p3/2$ $\alpha + {}^3\mathrm{He}$ phase shifts. The curves display results obtained from the effective-range expansion with parameters from Table I. Triangles $(p_{1/2})$ and circles $(p_{3/2})$ represent experimental values of Ref. [22]. The $p_{3/2}$ phase shifts are shifted by 90° for clarity.

TABLE I. Binding energy ϵ (MeV) and effective-range coefficients for lj partial waves of various collisions: scattering length a_{lj} (fm^{2l+1}), effective range r_{lj} (fm^{-2l+1}), and shape parameter P_{lj} (fm^{4l}). ANCs from the present analysis $(C_{lj}^{\rm eff})^2$ and ANCs deduced from experiment $(C_{lj}^{\rm exp})^2$ (fm^{-1}). In some lines, the ANC is obtained from the effective-range parameters of Ref. [8] (see text).

Collision	l	j	ϵ	a_{lj}	r_{lj}	P_{lj}	$(C_{lj}^{\rm eff})^2$	$(C_{lj}^{\rm exp})^2$
$^{16}O + p$	0	1/2	0.105	3708 ± 48	1.156 ± 0.005	-0.17 ± 0.36	5700	5700 ± 225 [18]
			0.65	815 [8]	1.16 [8]	-0.22 [8]	53.2	
			0.105	3828	1.16 [8]	-0.22 [8]	5850	
	2	5/2	0.60	1057 ± 27	-0.0804 ± 0.007	-365.6 ± 161.7	1.09	1.09 ± 0.11 [18]
$\alpha + t$	1	1/2	1.99	95.13 ± 1.73	-0.238 ± 0.007	39.18 ± 4.90	9.00	9.00 ± 0.90 [4]
			3.75	108.9 [8]	-0.22 [8]	56.99 [8]	7.70	
			1.99	90.1	-0.22 [8]	56.99 [8]	5.43	
	1	3/2	2.47	58.10 ± 0.65	-0.346 ± 0.005	9.86 ± 0.76	12.74	12.74 ± 1.10 [4]
			4.99	72.77 [8]	-0.27 [8]	26.59 [8]	16.47	
			2.47	69.9	-0.27 [8]	26.59 [8]	8.82	
$\alpha + {}^3He$	1	1/2	1.156	413 ± 7	-0.00267 ± 0.0028	$(2.66 \pm 8.39) \times 10^7$	15.9	15.9 ± 1.1 [19]
			2.88	665 [8]	-0.01 [8]	3.56×10^6 [8]	0.28	
	1	3/2	1.587	301 ± 6	-0.0170 ± 0.0026	$(9.69 \pm 4.69) \times 10^4$	23.2	23.2 ± 1.7 [19]
			3.99	253.1 [8]	-0.04 [8]	9212 [8]	4.79	

Other example: $^{14}N+p \rightarrow {}^{15}O+\gamma$

(PRC67(03)065804)

- $^{14}N(^{3}He,d)^{15}O$ at $E_{He3} = 26.3\ MeV$

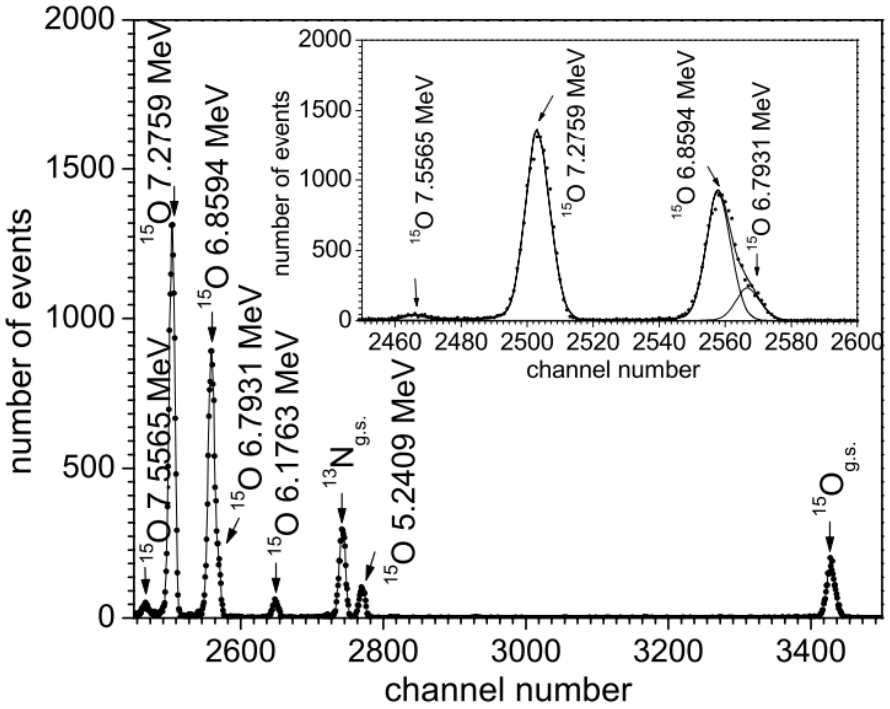

FIG. 1. Typical deuteron pulse height spectrum from the $^{14}N(^{3}He,d)^{15}O$ proton transfer reaction at 26.3 MeV, taken at a scattering angle $\theta_{LAB} = 15.5°$. The deconvolution of the 6.79+6.86 MeV doublet in ^{15}O is presented in the inset.

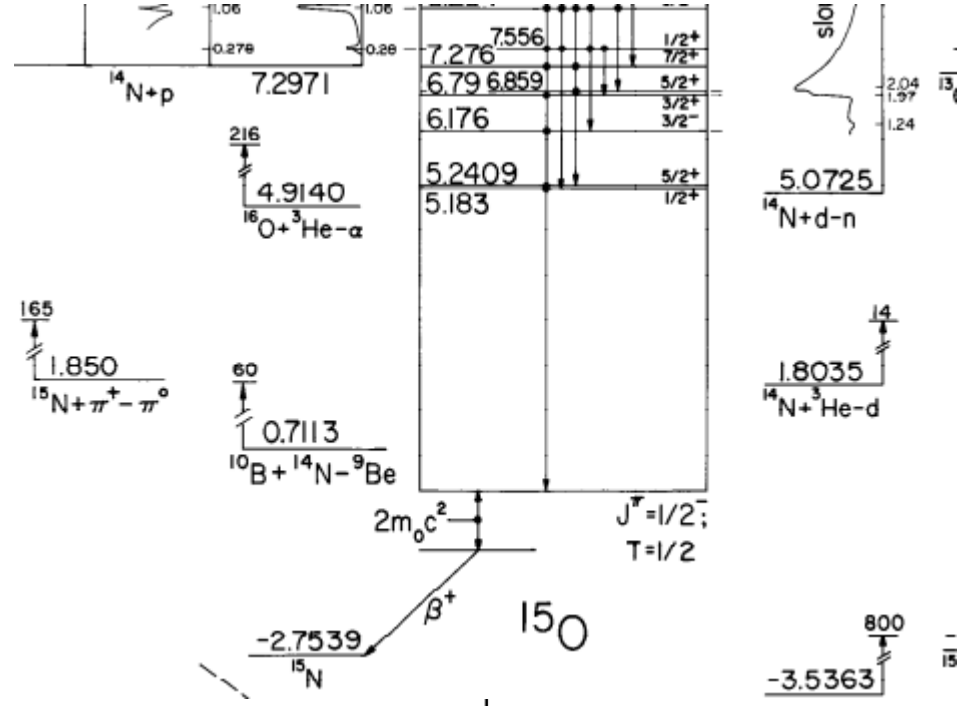

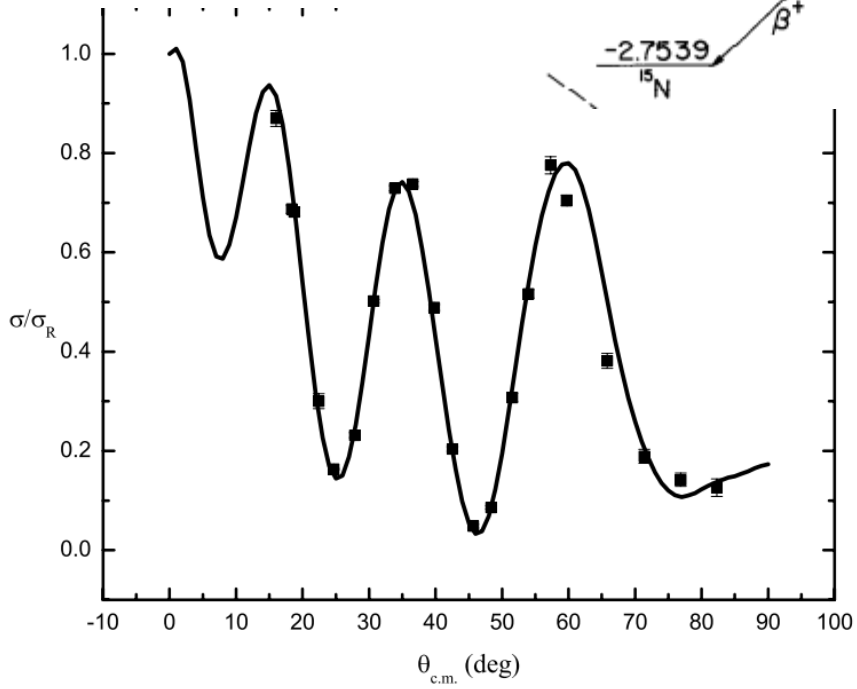

FIG. 2. Measured elastic scattering angular distribution for $^{14}N+{}^{3}He$ at 26.3 MeV, and the fit using optical potential P_i from

TABLE II. The ANCs for $^{14}\mathrm{N}+p\rightarrow{}^{15}\mathrm{O}$. J_f^π, E_f, are the spin parities and the excitation energies of the states in ^{15}O, given in the first column; the corresponding proton orbital and total angular momenta, l_f and j_f, are given in the second column. The ANCs (in fm^{-1}) determined here from the $^{14}\mathrm{N}(^3\mathrm{He},d)^{15}\mathrm{O}$ reaction are given in the third column, and those from Ref. [7] are given in the fourth column.

State ^{15}O	Proton orbitals	ANC	
J_f^π, E_f (MeV)	l_{fj_f}	C^2 (fm^{-1})	C^2 (fm^{-1})
$1/2^-$, 0.00	$p_{1/2}$	49.0 ± 5.4	63 ± 14[a]
	$p_{3/2}$	5.00 ± 0.55	
$5/2^+$, 5.24	$d_{5/2}$	0.11 ± 0.01	0.12 ± 0.03
$3/2^-$, 6.18	$p_{1/2}$	0.50 ± 0.06	0.46 ± 0.10
$3/2^+$, 6.79	$s_{1/2}$	24.0 ± 5.0	
	$d_{3/2}$	0.006 ± 0.001	
	$d_{5/2}$	0.01 ± 0.002	
$3/2^+$, 6.79	$s_{1/2}$	27.1 ± 6.8[b]	21 ± 5
	$d_{3/2}$	0.006 ± 0.002[b]	
	$d_{5/2}$	0.01 ± 0.003 [b]	0.080 ± 0.020
$5/2^+$, 6.86	$d_{5/2}$	0.32 ± 0.04	0.36 ± 0.08
$7/2^+$, 7.27	$d_{5/2}$	$(2.35\pm0.18)\times10^6$	$(2.7\pm0.6)\times10^6$

[a]The sum $C^2_{p_{1/2}}+C^2_{p_{3/2}}$.

[b]The ANC determined by us from the data in Ref. [7].

Possible future works by using ANC ?

$^{14}O(\alpha,\gamma)^{18}Ne$

- Can be addressed by $^{14}O(^{7}Li,t)^{18}Ne$?
- One may also measure $^{14}O(^{7}Li, \alpha)^{17}F$ for $^{14}O(\alpha, p)^{17}F$

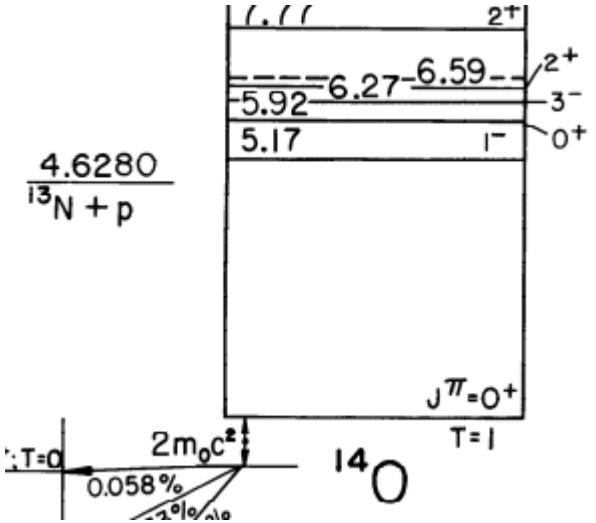

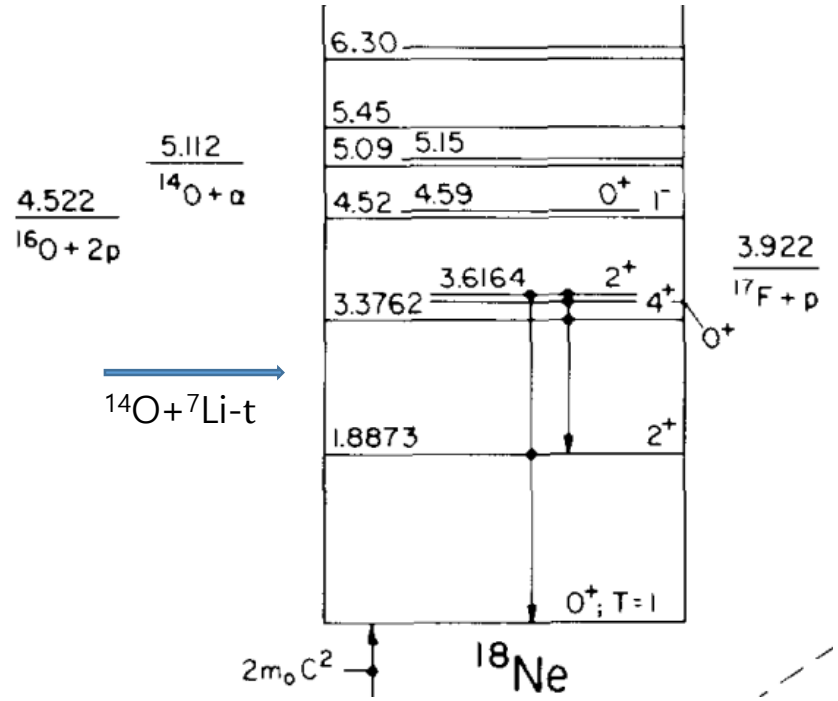

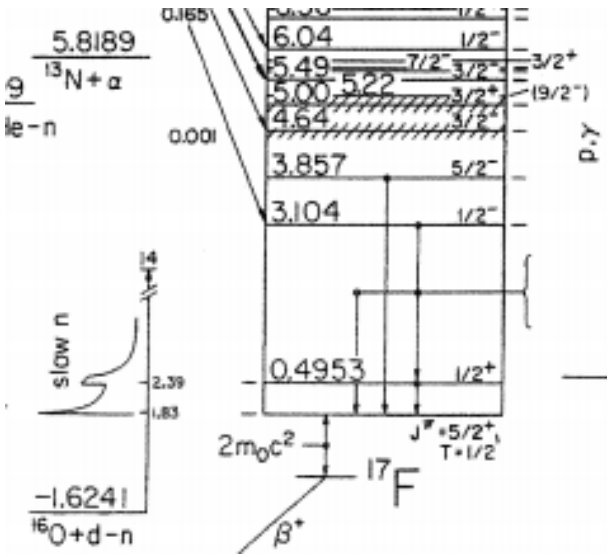

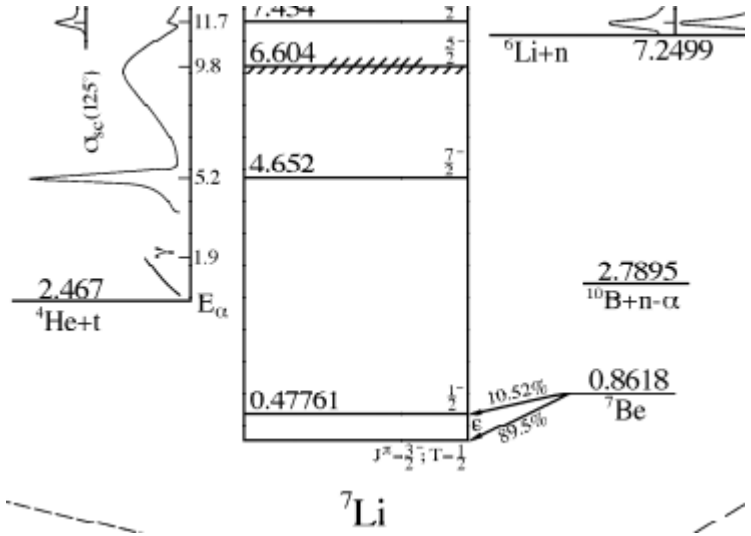

E_x (MeV ± keV)	J^π; T	τ or $\Gamma_{c.m.}$ (keV)
0	0^+; 1	$\tau_{1/2} = 1672 \pm 8$ msec
1.8873 ± 0.2	2^+	$\tau_m = 0.67 \pm 0.06$ psec
3.3762 ± 0.4	4^+	4.4 ± 0.6 psec
3.5763 ± 2.0	0^+	4 ± 2 psec
3.6164 ± 0.6	2^+	63^{+30}_{-20} fsec
4.519 ± 8	1^-	$\Gamma \leqslant 20$
4.590 ± 8	0^+	$\leqslant 20$
5.090 ± 8	$(2^+, 3^-)$	40 ± 20
5.146 ± 7	$(2^+, 3^-)$	25 ± 15

$^{15}O(\alpha,\gamma)^{19}Ne$ & $^{15}O(\alpha,p)^{18}F$

- Can be addressed by $^{15}O(^{7}Li,t)^{19}Ne$?

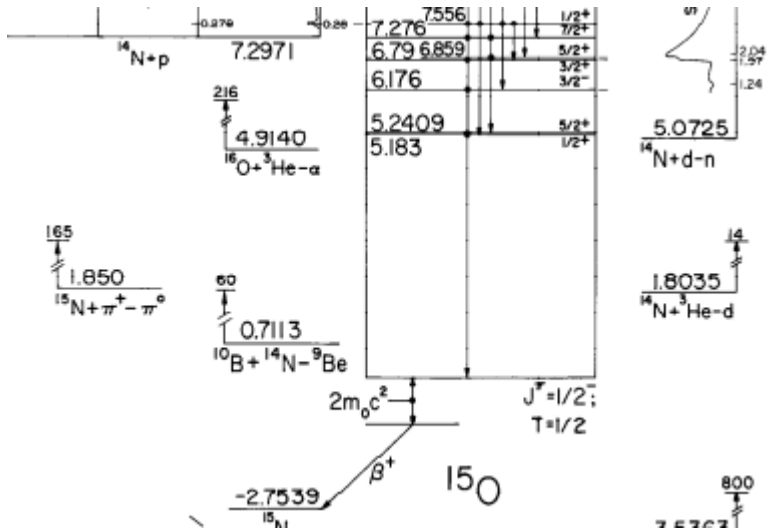

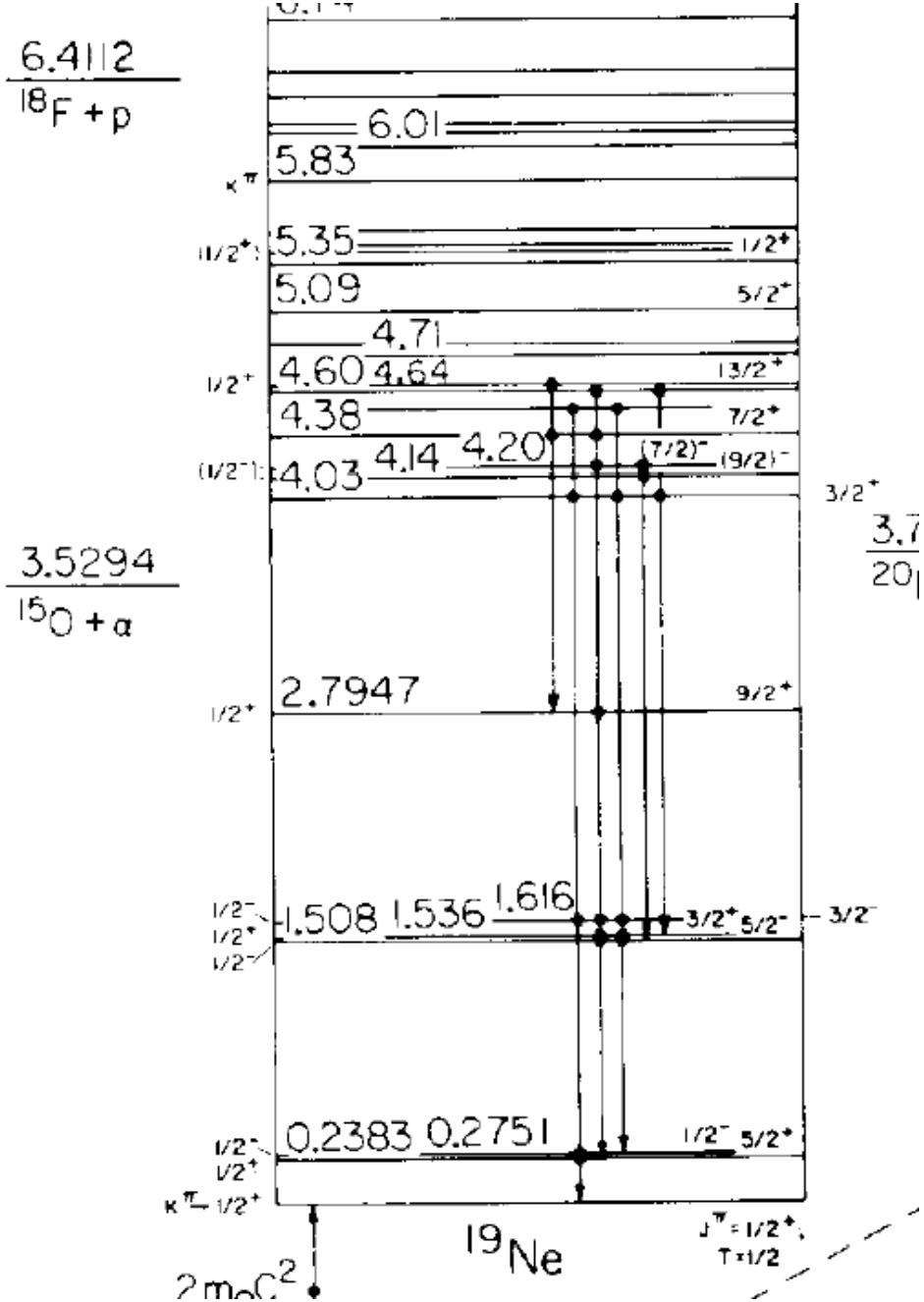

$$J^{\pi}(^{15}O) = {}^{1}/_{2}^{-}$$